Qiyuan Tan,[1,2] Monika Majewska-Szczepanik,[2,3] Xiaojun Zhang,[2] Marian Szczepanik,[2,3] Zhiguang Zhou,[1] F. Susan Wong,[4] and Li Wen[2]

IRAK-M Deficiency Promotes the Development of Type 1 Diabetes in NOD Mice

Type 1 diabetes mellitus (T1DM) is an organ-specific autoimmune disease characterized by progressive destruction of insulin-secreting pancreatic β-cells. Both T-cell–mediated adaptive responses as well as innate immune processes are involved in pathogenesis. Interleukin-1 receptor–associated kinase M (IRAK-M) can effectively inhibit the MyD88 downstream signals in Toll-like receptor pathways, while lack of IRAK-M is known to be associated with autoimmunity. Our study showed that IRAK-M–deficient (IRAK-M$^{-/-}$) nonobese diabetic (NOD) mice displayed early onset and rapid progression of T1DM with impaired glucose tolerance, more severe insulitis, and increased serum anti-insulin autoantibodies. Mechanistic studies showed that the enhanced activation and antigen-presenting function of IRAK-M$^{-/-}$ antigen-presenting cells from IRAK-M$^{-/-}$ mice were responsible for the rapid progression of disease. Moreover, IRAK-M$^{-/-}$ dendritic cells induced enhanced activation of diabetogenic T cells in vitro and the rapid onset of T1DM in vivo in immunodeficient NOD mice when cotransferred with diabetogenic T cells. This study illustrates how the modulation of innate immune pathways through IRAK-M influences the development of autoimmune diabetes.

The innate immune system recognizes foreign pathogens via germ-line–encoded receptors, termed pattern recognition receptors, which are mainly expressed on antigen-presenting cells (APCs) (1,2). Toll-like receptors (TLRs) are a well-described group of pattern recognition receptors that belong to the TLR/interleukin (IL)-1 receptor (IL-1R) superfamily (3). Beside effective pathogen clearance, excessive inflammatory responses caused by activating both the innate and adaptive immune systems though TLR engagement can lead to damage to self-tissues and development of autoimmune disease (4,5). IL-1R–associated kinase M (IRAK-M), also known as IRAK-3, is an inhibitor downstream of the MyD88-dependent pathway (6,7). Its expression inhibits cytokine production in monocytes and macrophages through modulating nuclear factor-κB (NF-κB) and the p38-mitogen-activated protein kinase (MAPK) pathway (6–9). The loss of IRAK-M expression in mice is linked with the development of sepsis, asthma, and pneumonia (10–12), as well as autoimmune diseases, including lupus, colitis, and inflammatory bowel disease (13–15).

Type 1 diabetes mellitus (T1DM) is an organ-specific autoimmune disease characterized by the progressive loss of insulin-producing pancreatic β-cells caused by T-cell–mediated autoimmune attack (16,17). Although adaptive immunity is clearly central to islet β-cell damage, the innate TLR signaling pathways are also involved in the development of autoimmune diabetes (18–22). IRAK-M function influences the development of autoimmune diseases (13–15), although the role of IRAK-M in autoimmune diabetes has not been previously defined. We report that IRAK-M–deficient (IRAK-M$^{-/-}$) NOD mice displayed early onset and rapid progression of autoimmune diabetes with enhanced autoimmune manifestations mediated by heightened inflammatory function of APCs in the absence of IRAK-M expression.

RESEARCH DESIGN AND METHODS

Mice

NOD/Caj and NOD.SCID mice were originally obtained from The Jackson Laboratory and have been maintained at Yale University for many years. IRAK-M$^{-/-}$ B6 mice were generated as previously described (6) and were obtained from The Jackson Laboratory. They were back-crossed onto the NOD genetic background for 10 generations with all *idd* markers determined by gene analysis. The genetic purity of the IRAK-M$^{-/-}$ NOD mice was further confirmed by mouse genome SNP analysis using Illumina GoldenGate genotyping assay (www.dartmouse org). The IRAK-M$^{+/+}$, IRAK-M$^{+/-}$, and IRAK-M$^{-/-}$ littermates used for diabetes investigation were obtained by inter-crossing IRAK-M$^{+/-}$ mice. BDC-2.5 NOD mice were obtained from The Jackson Laboratory and have been maintained at Yale University for about 8 years. All of the mice were kept in specific pathogen-free conditions in a 12-h dark/light cycle and were housed in individually ventilated filter cages with autoclaved food and bedding at the Yale University animal facility. The use of the animals and the procedures applied in this study were approved by the Institutional Animal Care and Use Committee of Yale University.

Natural History of Diabetes Development

The incidence of diabetes was observed in IRAK-M$^{+/+}$, IRAK-M$^{+/-}$, and IRAK-M$^{-/-}$ female and male littermates by weekly screening for urine glucose. Diabetes was confirmed by glycosuria and blood glucose levels ≥250 mg/dL (13.9 mmol/L).

Antibodies and Reagents

All the fluorochrome-conjugated monoclonal antibodies (mAbs) used in this study were purchased from eBioscience or BioLegend. Alkaline phosphatase–conjugated goat anti-mouse IgG (goat anti-mouse IgG-AP) for ELISA was purchased from Southern Biotechnology, and phosphatase substrate was purchased from Sigma. Hybridoma supernatants containing mAbs, used for cell purification or stimulation, were generously provided by the late Charles Janeway Jr. (Yale University). Magnetic beads conjugated with goat anti-mouse IgG, goat anti-mouse IgM, or goat anti-rat IgG were purchased from Qiagen. RPMI-1640 medium and heat-inactivated FCS were purchased from Invitrogen and Gemini, respectively. The BDC-2.5 mimotope peptide (RTRPLWVRME) was synthesized at the Keck Foundation Biotechnology Resource Laboratory of Yale University.

Intraperitoneal Glucose Tolerance Test

Mice were fasted overnight (free access to water) prior to intraperitoneal injection of glucose (2 mg/g body weight), and blood glucose was measured at different time points after glucose challenge.

Histopathology and Insulitis Score

Pancreata were fixed in 10% buffered formalin and then embedded in paraffin. Tissues were sectioned and stained with hematoxylin-eosin. Insulitis was scored under light microscopy with the following grading scale: 0, no insulitis; 1, insulitis affecting 25% of the islet; 2, insulitis affecting 25–75% of the islet; and 3, insulitis affecting >75% of the islet. A range of 182–209 islets were scored for insulitis in each group (*n* = 7–8 mice).

Serum Anti-Insulin Autoantibody Detection (ELISA)

The concentration of anti-insulin IgG was measured in serum samples from 3-month-old female IRAK-M$^{-/-}$ NOD mice and wild-type (WT) NOD mice. Plates were coated with human insulin (10 μg/mL; Lilly) overnight, and 1:100 diluted serum samples were tested for anti-insulin IgG by ELISA with goat anti-mouse IgG-AP (Southern Biotechnology) and phosphatase substrate (Sigma). The ELISA plates were read by microplate spectrophotometer at an optical density of 405 nm.

Cell Purification

After removing B cells (using anti-mouse Ig) and other APCs (I-A^{g7} major histocompatibility complex [MHC] class II$^+$) using anti-I-A^{g7} (10.2.16) mAb and magnetic bead separation, CD4$^+$ or CD8$^+$ T cells were purified by magnetic bead–based negative selection using the anti-CD8 (T1B105) or anti-CD4 (GK1.5) mAb, respectively. The purity of the isolated T cells used for adoptive transfer experiments was routinely ≥90%, analyzed by flow cytometry. Dendritic cells (DCs) were purified by CD11c-positive selection kit (Stem Cell Technology).

Carboxyfluorescein Diacetate Succinimidyl Ester–Labeled Cell Proliferation Assay

Purified splenic CD4$^+$ BDC-2.5 T cells were labeled with carboxyfluorescein diacetate succinimidyl ester (CFSE) and 5 × 10^6 cells/mouse were intravenously injected into IRAK-M$^{-/-}$ NOD mice and WT NOD mice. Recipient mice were killed 3 days later, and lymphocytes from spleen and pancreatic lymph nodes (PLNs) were harvested and stained with anti-CD4, and CFSE dilution was examined by flow cytometry.

Adoptive Transfer Experiments

In the total immune cell adoptive transfer experiments, 10^7 splenocytes were harvested from newly diagnosed diabetic IRAK-M$^{-/-}$ NOD or WT NOD female mice and injected intravenously into ~5-week-old NOD.SCID mice. In an APC adoptive transfer model, 5 × 10^6 magnetic-bead purified APCs (depleted of CD4$^+$ and CD8$^+$ T cells) from IRAK-M$^{-/-}$ NOD or WT NOD female mice were cotransferred with 2 × 10^6 magnetic bead–purified BDC-2.5 CD4$^+$ T cells to 4- to 5-week-old NOD.SCID mice. Purified BDC-2.5 CD4$^+$ T cells alone were also transferred to the NOD.SCID mice as controls to test the effect of endogenous APCs in NOD.SCID mice. In DC adoptive transfer experiments, purified CD11c$^+$ DCs from IRAK-M$^{-/-}$ NOD or WT NOD female mice were preloaded with BDC-2.5 mimotope (500 ng/mL) in complete medium at 37°C for 5 h, followed by washing with PBS (twice). A total of 10^6 DCs were then cotransferred with 2 × 10^6

BDC-2.5 CD4^{+} T cells into 4- to 5-week-old NOD.SCID mice. Diabetes development was monitored in all recipients by weekly screening for urine glucose levels, and diabetes was confirmed by glycosuria and blood glucose levels ≥250 mg/dL (13.9 mmol/L).

Intracellular Cytokine Assay

Lymphoid cells were first stimulated with phorbol myristic acid (50 ng/mL; Sigma) and ionomycin (500 ng/mL; Sigma) in the presence of Golgi Plug (eBioscience) at 5×10^6/mL in cell culture medium for 4 h. The intracellular cytokine staining (ICC) was performed according to the protocol provided with kits from eBioscience. The cells were stained with surface markers before fixation and permeabilization. Fc receptors were blocked with 2.4G2 Fc-blocking antibody before staining with the recommended amount of fluorochrome-labeled antibody for the detection of intracellular cytokines.

Bone Marrow–Derived DC Culture

Bone marrow cells were flushed from the tibia of either IRAK-M^{−/−} NOD or WT NOD mice. Cells were resuspended by repeated pipetting in culture medium, and erythrocytes were lysed before the culture. Bone marrow cells were then counted and seeded in 60-mm culture dishes at a density of 1.5×10^6/mL in DC differentiation medium (RPMI-1640 complete medium) with 5% FCS, 20 ng/mL mouse IL-4 (Biolegend), and 20 ng/mL mouse GM-CSF (Biolegend) for 7 days at 37°C. Culture medium was replenished every other day. Cells were harvested on day 7, were analyzed by flow cytometry after staining with CD11b and CD11c, and >90% of cells were CD11c^{+}, which were considered to be bone marrow–derived DCs (BMDCs).

Western Blot Analysis

BMDCs from IRAK-M^{−/−} NOD or WT NOD mice were stimulated with or without lipopolysaccharide (LPS; 1 μg/mL). BMDCs were harvested at 15, 30, or 60 min after the stimulation, and were washed with cold PBS three times followed by resuspending in cell-lysing buffer containing protease and phosphatase inhibitor. The protein concentration in the cell lysates was measured by BCA protein assay kit (Pierce), and 30 μg/lane protein was used for blotting. After blocking with 5% BSA/PBS, the blots were incubated with primary antibodies overnight (phospho-extracellular signal–related kinase [ERK]1/2, ERK1/2, NFκB-phospho p65, and actin, all from Cell Signaling Technology) followed by different horseradish peroxidase–conjugated secondary antibodies (Cell Signaling Technology or Pierce) for 1 h. The blots were placed on X-ray film (Denville) and developed with a chemiluminescent horseradish peroxidase antibody detection kit (Denville).

Luminex Assay to Determine Cytokines

Culture supernatants from a culture of splenic DCs (5×10^5/well) with or without stimulation by TLR ligands (LPS 1 μg/mL, CPG 1 μg/mL, or Pam_3CSK_4 1 μg/mL) for 12 h) were harvested, and secreted IL-6, IL-12p40, IL-1β, and interferon (IFN)-γ were measured by Luminex following the manufacturer's protocol (Bio-Rad). Secreted IFN-γ, IL-6, and IL-1β were also measured by Luminex from a T cell-DC coculture supernatant, where T cells were activated with anti-CD3 (1:300 2C11 hybridoma medium) for 4 days. Luminex plates were read on a Luminex reader (Bio-Plex 200; Bio-Rad).

Immunization or DC Vaccine Experiments

NOD mice were injected intraperitoneally with keyhole limpet hemocyanin (KLH; Sigma), 200 μg/mouse as a foreign antigen, and were emulsified in Alum (Pierce). Mice were killed 7 days after immunization, and CD4^{+} and CD8^{+} T cells were isolated from the splenocytes by magnetic bead–based negative selection. DCs were purified from IRAK-M^{−/−} and WT NOD mice by a CD11c positive selection kit (Stemcell Technologies). DCs were or were not loaded with KLH (Sigma) 50 μg/mL for 5 h in complete medium at 37°C. Antigen-loaded DCs were then washed with PBS twice before coculturing with T cells. CD4^{+} and CD8^{+} T cells from immunized mice were cocultured with DCs from IRAK-M^{−/−} NOD or WT NOD mice, with or without KLH, at a 2:1 ratio in complete medium. ^{3}H-thymidine was added during the last 16 h of a 5-day culture, to determine antigen-specific T-cell proliferation responses by ^{3}H-thymidine incorporation. In DC vaccine experiments, purified DCs from immunized mice were preloaded with KLH, as described above, and 10^6 cells were injected intravenously into WT NOD mice. The mice were killed 7 days after DC vaccination, and splenocytes were harvested and placed 10^5/well with KLH (1 μg/mL) in complete medium. Proliferative responses were determined by ^{3}H-thymidine incorporation. ^{3}H-thymidine was added during the last 16 h of a 5-day culture.

Statistical Analysis

Statistical analysis was performed using GraphPad Prism software. Diabetes incidence was compared using the Gehan-Breslow-Wilcoxon test. In vitro assays were analyzed with a Student t test or ANOVA, and $P < 0.05$ was considered to be significant.

RESULTS

IRAK-M Deficiency Promotes T1DM Development in NOD Mice

To determine the role of IRAK-M in autoimmune diabetes, we generated IRAK-M^{−/−} NOD mice by crossing IRAK-M^{−/−} B6 mice onto the NOD genetic background, the purity of which was analyzed by single nucleotide polymorphism (SNP) scanning of the whole mouse genome (Supplementary Fig. 1). We observed diabetes development in IRAK-M^{−/−} NOD mice and compared it with development in IRAK-M^{+/−} and IRAK-M^{+/+} littermates over 32 weeks. We found that the female IRAK-M^{−/−} NOD mice developed diabetes as early as 6–7 weeks with a higher total incidence compared with onset at 11 and 14 weeks, respectively, in IRAK-M^{+/−} and IRAK-M^{+/+} littermates (Fig. 1A). There was no significant difference in diabetes
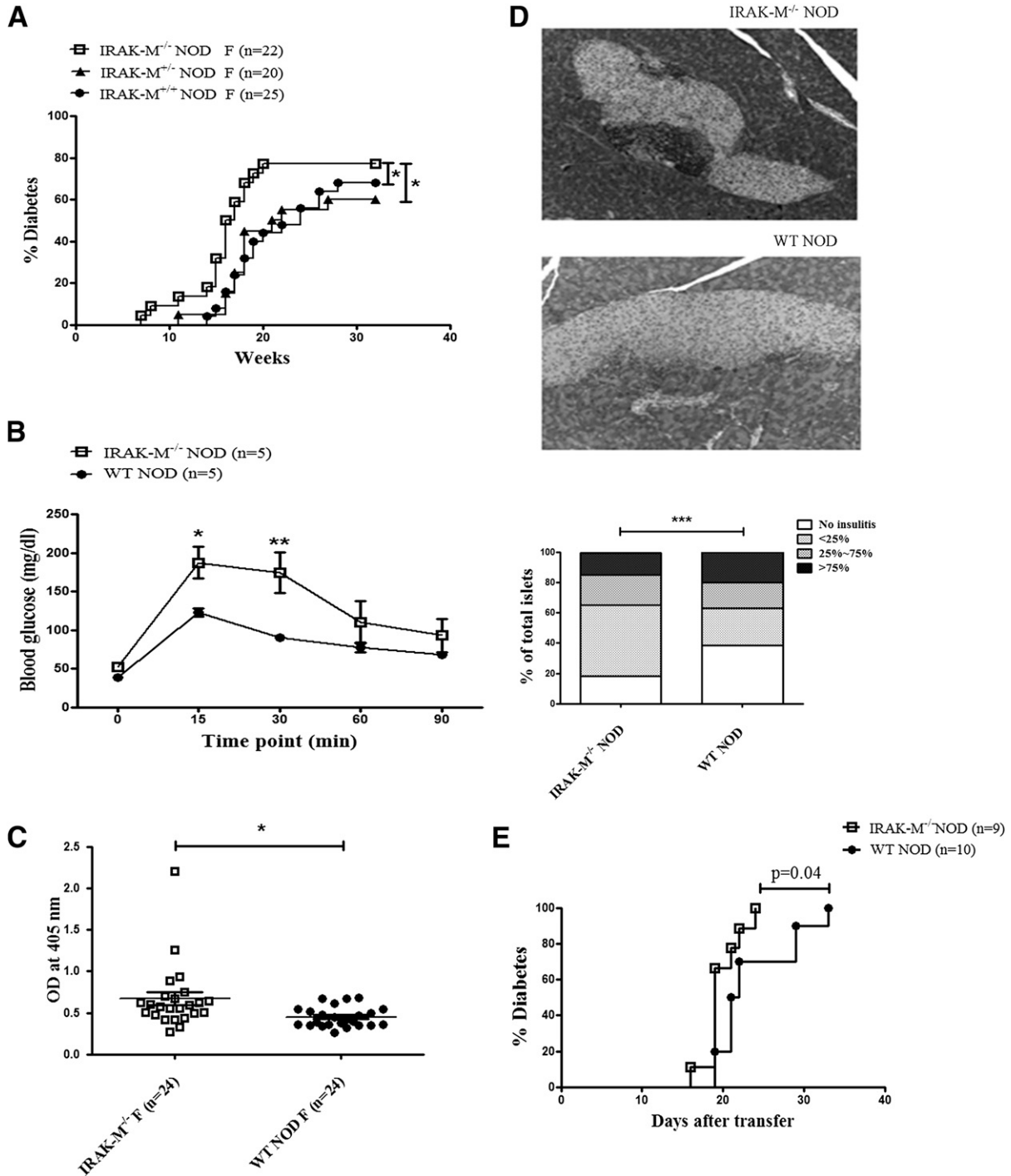
Figure 1—IRAK-M deficiency promotes the development of T1DM in NOD mice. *A*: Diabetes incidence in female IRAK-M$^{-/-}$ NOD and IRAK-M$^{+/-}$ NOD mice, and their WT NOD littermates. Statistical analysis was performed by Gehan-Breslow-Wilcoxon test. *B*: An intraperitoneal glucose tolerance test was performed in ~12-week-old female IRAK-M$^{-/-}$ NOD and WT NOD mice that were fasted overnight with free access to water. Blood glucose was measured at the indicated time points after glucose injection (2 g/kg body weight i.p.; *n* = 5 mice/group), and data were analyzed by two-way ANOVA. *C*: Serum anti-insulin IgG was measured in serum samples of 12-week-old nondiabetic female IRAK-M$^{-/-}$ NOD and WT NOD mice by ELISA (*n* = 24/group). Data are presented as an optical density (OD) of 405 nm and were analyzed by Student *t* test. *D*: Histology of islet infiltration in 12-week-old nondiabetic female IRAK-M$^{-/-}$ NOD and WT NOD mice. Hematoxylin-eosin staining of the pancreas showed more immune cell infiltration in islets of IRAK-M$^{-/-}$ NOD mice compared with the control mice (top). Insulitis was quantified using the following scoring system: 0, no insulitis; 1, <25% infiltration; 2, 25–75% infiltration; 3, >75% infiltration (bottom). Seven to eight mice were examined in each group, and insulitis was scored in 182–209 islets/group. Statistical analysis was performed with χ^2 test. *E*: Splenocytes from diabetic female IRAK-M$^{-/-}$ NOD or WT NOD mice were transferred into 4- to 5-week-old NOD.SCID mice (*n* = 9–10/group), and the incidence of diabetes was investigated. NOD.SCID mice that received IRAK-M$^{-/-}$ NOD splenocytes had a more rapid onset of diabetes. *P < 0.05; **P < 0.001; ***P < 0.0001.

development in the males of the different genotypes, although male IRAK-M$^{-/-}$ NOD mice also had a trend toward early diabetes onset (data not shown). To test β-cell function, which was determined by insulin secretion in response to glucose challenge in vivo, we performed intraperitoneal glucose tolerance tests at a prediabetic stage in nondiabetic female mice (random nonfasting blood glucose level <150 mg/dL) after fasting over 12 h. Blood glucose levels of IRAK-M$^{-/-}$ NOD mice were significantly higher at both 15-min ($P < 0.05$) and 30-min ($P < 0.001$) time points after glucose injection (Fig. 1*B*). We also examined anti-insulin IgG autoantibody (IAA) production, an important indicator of humoral autoimmune responses in T1DM, and found increased levels of IAA in the serum of female IRAK-M$^{-/-}$ NOD mice compared with WT NOD counterparts (Fig. 1*C*) ($P = 0.011$). Next, we analyzed the insulitis score of female IRAK-M$^{-/-}$ and WT NOD mice. Although there were more islets with severe insulitis (infiltration >75%) in WT NOD mice compared with the IRAK-M$^{-/-}$ NOD mice (19.7% vs. 14.8%), the total number of infiltrated islets was much higher in the IRAK-M$^{-/-}$ group compared with the WT group (81.6% vs. 61.4%), as determined by insulitis score (Fig. 1*D*) ($P < 0.0001$). To investigate whether IRAK-M deficiency could enhance the diabetogenicity of immune cells, we adoptively transferred splenocytes (intravenously) from diabetic IRAK-M$^{-/-}$ NOD or WT NOD mice to NOD.SCID mice (10^7/mouse). In line with the natural history of diabetes development in IRAK-M$^{-/-}$ NOD mice, NOD.SCID mice that received IRAK-M$^{-/-}$ NOD splenocytes also developed accelerated diabetes compared with the NOD. SCID mice injected with WT NOD splenocytes (Fig. 1*E*) ($P < 0.05$). To further confirm the enhanced role of IRAK-M in T1DM development, we also adoptively transferred splenocytes from diabetic WT NOD mice to irradiated IRAK-M$^{-/-}$ or WT NOD recipients. Again, the onset of diabetes in IRAK-M$^{-/-}$ NOD mice was much faster than in their WT counterparts (day 14 vs. day 35; data not shown). Taken together, these data revealed that IRAK-M, as a negative regulator of TLR signaling, is important in protecting against T1DM in NOD mice because, in the absence of IRAK-M, NOD mice had impaired glucose tolerance, a higher level of IAA, more inflamed islets, and a faster onset of diabetes, both spontaneously or adoptively transferred.

IRAK-M$^{-/-}$ NOD Mice Showed Enhanced T-Cell Activation and Proinflammatory Cytokine Production

It is known that both pathogenic CD4$^+$ and CD8$^+$ T cells infiltrate into the pancreatic islets and mediate islet β-cell damage. To uncover the mechanism by which IRAK-M influences the process, we first examined T-cell phenotype. As shown in Fig. 2*A* and *B*, splenic T cells from 3-month-old female IRAK-M$^{-/-}$ NOD mice had a significantly higher proportion of effector/memory cells (CD44^{hi}CD62L^{lo}) compared with WT NOD mice ($P = 0.002$ for CD4$^+$ T cells; $P = 0.02$ for CD8$^+$ T cells), and proportionally reduced naive CD4$^+$ and CD8$^+$ T cells (CD44^{lo}CD62L^{hi}) compared with WT NOD mice, although the reduction was not statistically significant (Fig. 2*A* and *B*). The same pattern was found in pancreatic draining lymph nodes (Supplementary Fig. 2). We then examined intracellular cytokine profiles of T cells from IRAK-M$^{-/-}$ and WT NOD mice. We found that there were more IFN-γ–producing CD4$^+$ T cells ($P = 0.044$) and more tumor necrosis factor-α (TNF-α)-producing CD8$^+$ T cells ($P = 0.015$) in splenocytes of IRAK-M$^{-/-}$ NOD mice compared with WT NOD mice (Fig. 2*C* and *D*). The frequency of proinflammatory cytokine–producing CD4$^+$ T cells was also significantly higher in the PLNs of IRAK-M$^{-/-}$ NOD mice compared with WT NOD mice ($P < 0.05$ for IFN-γ; $P < 0.01$ for TNF-α). Interestingly, the frequency of proinflammatory cytokine–producing CD8$^+$ T cells from PLNs was similar between the two strains. We also studied the number of IL-10–producing CD4$^+$ T cells and Foxp3$^+$ regulatory T cells from both the spleen and PLNs. The frequency of IL-10–producing CD4$^+$ T cells in IRAK-M$^{-/-}$ NOD mice was lower than that in WT NOD mice, but this was not statistically significant (data not shown). It is interesting that the number of regulatory T cells was comparable in both strains (data not shown). Our data revealed that there were more effector/memory T cells in IRAK-M$^{-/-}$ NOD mice, which produced more inflammatory cytokines than WT NOD mice.

APCs Lacking IRAK-M Expression Have a More Activated Phenotype and Enhanced Diabetogenic Function

APCs play a pivotal role in activating T cells, including diabetogenic T cells, through processing and presenting self-antigens. Because IRAK-M is mostly expressed in APCs, including monocytes, macrophages (6,8,23), and B cells (24), we tested whether APCs lacking IRAK-M expression were responsible for promoting the accelerated diabetes seen in IRAK-M$^{-/-}$ NOD mice. As shown in Fig. 3*A* and *B*, we found that in IRAK-M$^{-/-}$ NOD mice compared with WT NOD mice (all females, 3 months old), a higher number of CD11b$^+$ macrophages and CD11c$^+$ DCs expressed the activation/costimulatory marker CD80 (CD11b$^+$ cells $P < 0.01$; CD11c$^+$ cells $P < 0.01$), CD86 (CD11b$^+$ cells $P < 0.01$; CD11c$^+$ cells $P < 0.05$) as well as MHC class II molecules (CD11b$^+$ cells $P < 0.05$; CD11c$^+$ cells $P < 0.05$).

Next, we examined inflammatory cytokine production in these APCs in IRAK-M$^{-/-}$ and WT NOD mice. Our results showed, in IRAK-M$^{-/-}$ NOD mice compared with WT NOD mice, higher numbers of IFN-γ–producing CD11b$^+$ macrophages and CD11c$^+$ DCs (CD11b$^+$ cells $P = 0.0017$; CD11c$^+$ cells $P = 0.0010$; Fig. 3*C*). Moreover, there was a significantly higher frequency of IL-6–producing and IL-12–producing CD11c$^+$ cells in IRAK-M$^{-/-}$ NOD mice (Fig. 3*D*; IL-6 $P < 0.05$; IL-12 $P < 0.05$). There were higher numbers of IL-6–producing and IL-12–producing CD11b$^+$ cells as well, but the increase was not
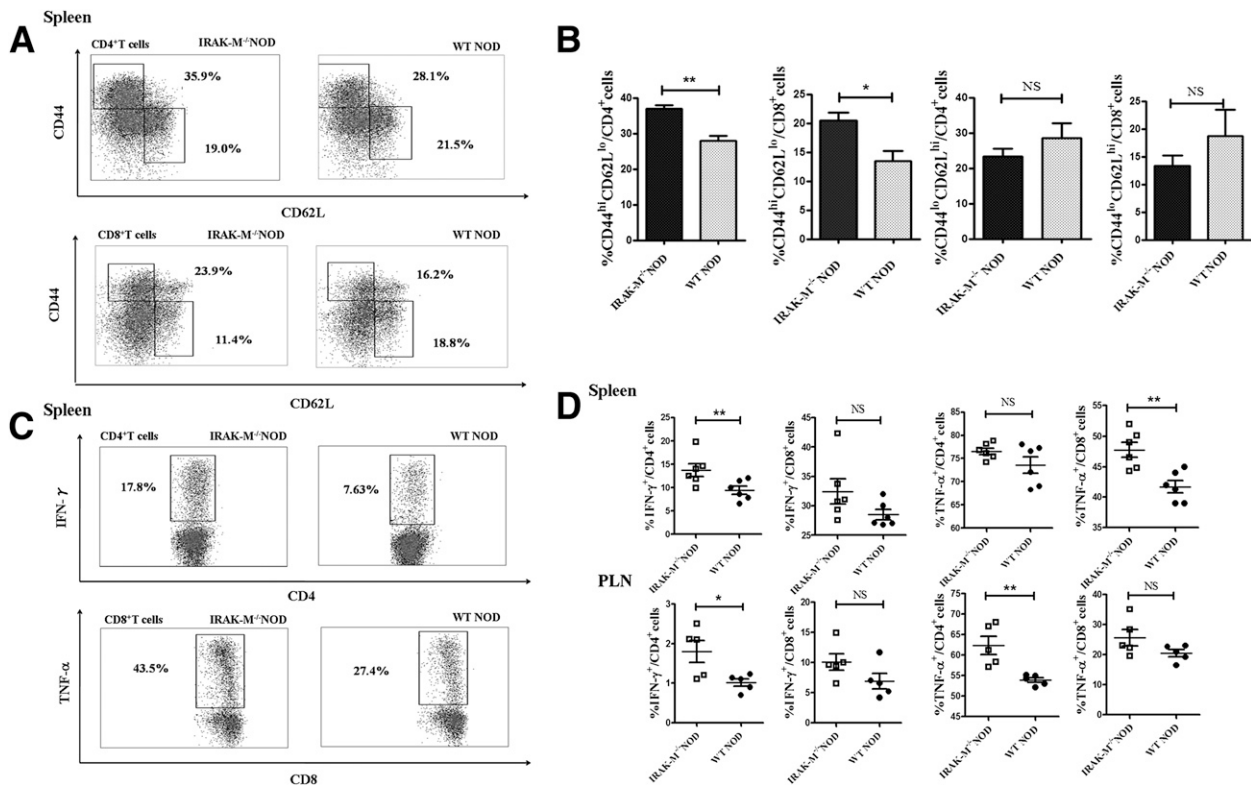
Figure 2—T-cell hyper-reactivity in IRAK-M$^{-/-}$ NOD mice. A: Splenocytes from IRAK-M$^{-/-}$ NOD and WT NOD mice were stained for CD44 and CD62L expression in gated CD4$^+$ or CD8$^+$ T cells. B: Summary of effector/memory (CD44^{high}CD62L^{low}) and naive (CD44^{low}CD62L^{high}) T cells in total CD4$^+$ or CD8$^+$ T cells in IRAK-M$^{-/-}$ NOD and WT NOD mice (n = 4 mice/group). C: Splenocytes and draining PLN cells were stained for intracellular IFN-γ and TNF-α in CD4$^+$ and CD8$^+$ T cells, and analyzed by flow cytometry. Flow cytometric plots of splenic IFN-γ–expressing cells were shown in gated CD4$^+$ or CD8$^+$ cells. D: Summary of the percentage of IFN-γ$^+$ and TNF-α$^+$ cells in CD4$^+$ and CD8$^+$ T-cell populations in spleen and PLNs. Data represent at least three individual experiments. The Student t test was used for statistical analysis. *P < 0.05; **P < 0.001. NS, not significant.

statistically significant (data not shown). These results suggest that, in the absence of IRAK-M, APCs are more activated and produce more type 1 T-helper cell (Th1)–driven cytokines, which might perturb the development of immune tolerance.

To test the above possibility, we studied the function of APCs in vivo and used diabetogenic BDC-2.5 CD4$^+$ T cells, which respond to chromogranin A and are highly pathogenic (25). Purified BDC-2.5 CD4$^+$ T cells from BDC-2.5 TCR transgenic NOD mice were labeled with CFSE and injected intravenously into IRAK-M$^{-/-}$ NOD or WT NOD mice. The proliferation of BDC-2.5 T cells in the PLNs, determined by CFSE dilution, was used as an indicator for APC function. Interestingly, we found that 3 days after injection, more BDC-2.5 T cells proliferated into the PLNs of IRAK-M$^{-/-}$ NOD mice than into WT NOD mice (P < 0.05; Fig. 4A). This was not obvious in the spleen (P = 0.09; Fig. 4A). We then took a direct approach, transferring purified BDC-2.5 CD4$^+$ T cells (2 × 10^6/mouse) together with APCs (T-cell–depleted splenocytes 5 × 10^6/mouse) from either IRAK-M$^{-/-}$ NOD or WT NOD mice to NOD.SCID recipients and observed the mice for diabetes development. Supporting our in vivo proliferation data, we found that NOD.SCID mice that

received IRAK-M$^{-/-}$ APCs developed diabetes more rapidly than the recipients that received WT APCs (Fig. 4B; P = 0.04) in an observation period of 40 days. To exclude the role of endogenous APCs in NOD.SCID recipients, we transferred purified BDC-2.5 CD4$^+$ T cells (2 × 10^6/mouse) without exogenous APCs to an additional group of NOD.SCID mice, and the incidence of diabetes in this control group was similar to that in the mice that received APCs from WT NOD mice (Fig. 4B; P = 0.08), but there was a significant difference compared with the group cotransferred with IRAK-M$^{-/-}$ APCs (Fig. 4C; P = 0.02). Our data suggest that, in the absence of IRAK-M, APCs significantly facilitate the destruction of islet β-cells by the pathogenic T cells.

Phenotype and Function of DCs in the Presence and Absence of IRAK-M

DCs are the most potent APCs that initiate adaptive immune responses (26). As IRAK-M negatively regulates MyD88, a "master" adaptor molecule of many TLR downstream signaling pathways, we first tested whether IRAK-M removal could alter the activation and cytokine production of DCs by TLR ligation. We examined the phenotype and function of splenic DCs after stimulation with
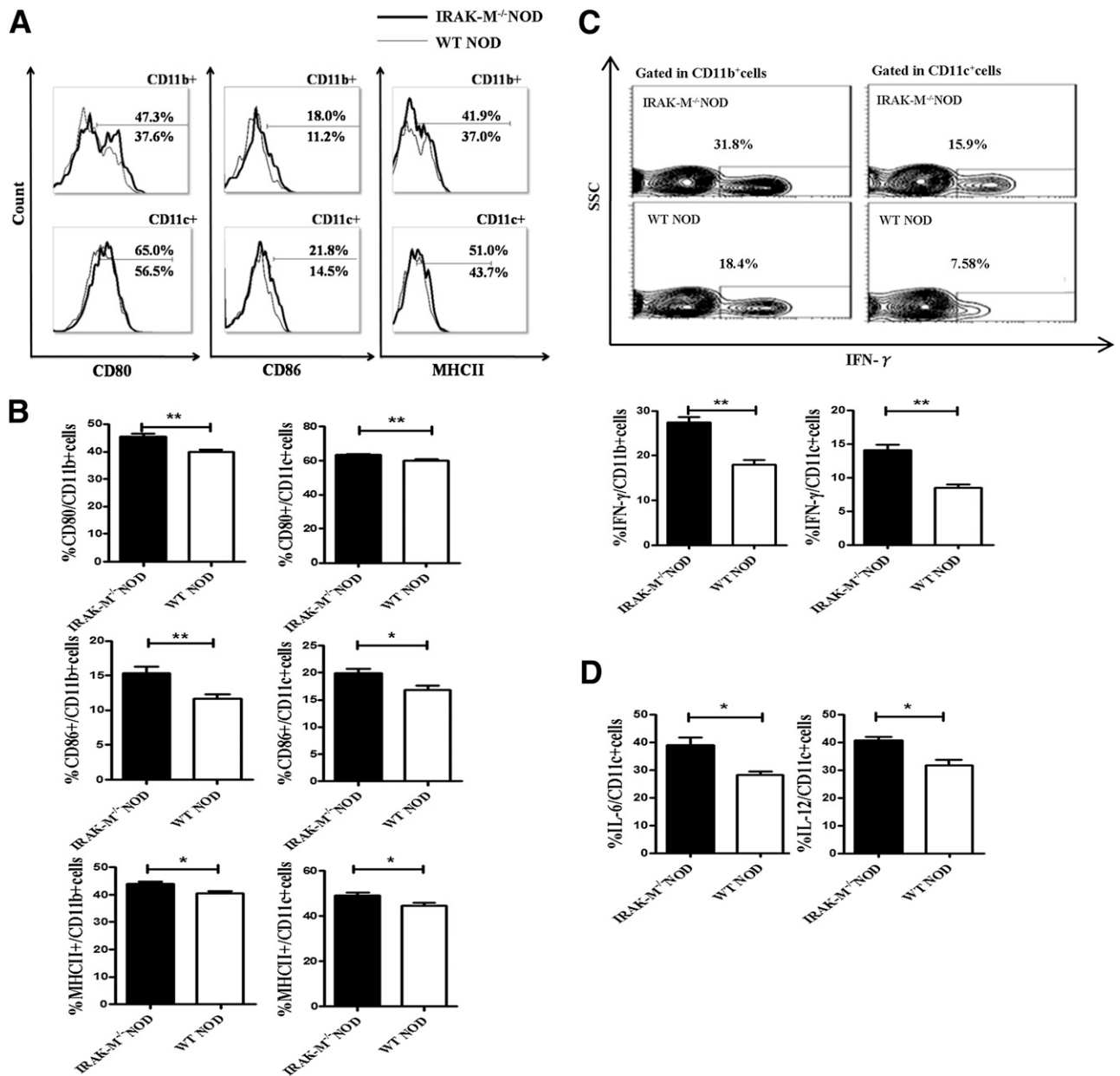
Figure 3—More DCs and macrophages in IRAK-M$^{-/-}$ NOD mice expressed inflammatory cytokine and maturation markers. Representative histograms of CD80, CD86, and MHC class II expression in splenic CD11b$^+$ macrophages and CD11c$^+$ DCs are shown (A), and percentages of positive cells are summarized (B). Bold line: IRAK-M$^{-/-}$ NOD; thin line: WT NOD. Data are representative of three experiments. C and D: Splenocytes from IRAK-M$^{-/-}$ NOD and WT NOD mice were examined for the expression of IFN-γ, IL-6, and IL-12 in CD11c$^+$ and CD11b$^+$ cells by intracellular cytokine staining after 4 h of stimulation with phorbol myristic acid and ionomycin, and were analyzed by flow cytometry (n = 4–6 mice/group). Production of IFN-γ was significantly increased in splenic CD11c$^+$ and CD11b$^+$ cells in IRAK-M$^{-/-}$ NOD mice. Representative flow cytometric contour plots are shown in the top panel of C, and the summary of IFN-γ^+ cells are shown in the bottom panel of C. D: The levels of IL-6 and IL-12 are shown in gated CD11c$^+$ cells. Data shown are representative of at least three experiments. Statistical analysis was performed using Student t test: *$P < 0.05$; **$P < 0.001$.

different TLR agonists including LPS (TLR4; Sigma), cytosine guanine dinucleotide (CpG [TLR9]; InvivoGen), Pam$_3$CSK$_4$ (TLR2; InvivoGen), and polyinosinic:polycytidylic acid (poly I:C [TLR3]; Sigma). Similar to the results seen in unstimulated DCs (Fig. 3A and B), a higher percentage of DCs from IRAK-M$^{-/-}$ NOD mice expressed activation and costimulatory molecules compared with DCs from WT NOD mice in response to LPS, CpG, or

Pam$_3$CSK$_4$, but not poly I:C (Fig. 5A). The unresponsiveness to poly I:C stimulation might be explained by the fact that poly I:C activates TLR3, which signals through the TIR-domain–containing adaptor-inducing IFN-β (TRIF) but not the MyD88 pathway. It is noteworthy that more DCs from IRAK-M$^{-/-}$ NOD mice expressed activation and costimulatory molecules compared with DCs from WT NOD mice even without stimulation by TLR
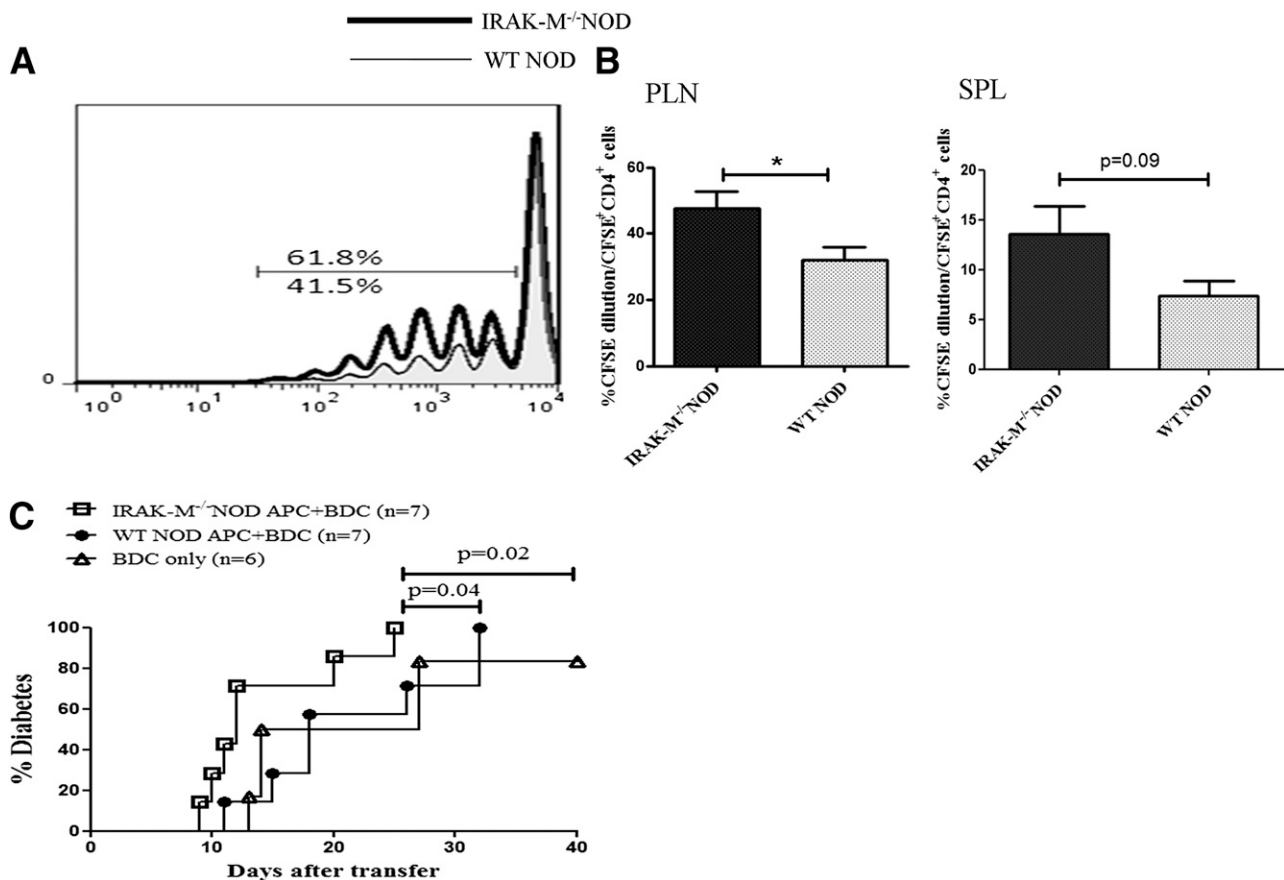
Figure 4—IRAK-M$^{-/-}$ APCs promoted diabetogenic T-cell proliferation and diabetogenicity in vivo. A and B: 5×10^6 magnetic bead–purified CD4$^+$ T cells were labeled with CFSE (5 nmol/L) and injected intravenously into IRAK-M$^{-/-}$ NOD and WT NOD mice (3–4 mice/group). Mice were killed 3 days after injection, and CD4$^+$ T cells in PLNs were analyzed for CFSE dilution by flow cytometry. A: A representative histogram plot shows CFSE dilution of BDC-2.5 CD4$^+$ T cells. B: Summary of CFSE-diluted BDC-2.5 CD4$^+$ T cells in PLN and spleen cells. Data were analyzed by Student t test and represent two individual experiments (*P < 0.05). C: Magnetic bead–purified BDC-2.5 CD4$^+$ T cells (2×10^6/mouse) together with bead-purified APCs (bead-depleted CD4$^+$ and CD8$^+$ T cells, 5×10^6/mouse) from either IRAK-M$^{-/-}$ NOD or WT NOD mice were injected into NOD.SCID mice (4–5 weeks old). NOD.SCID mice that received BDC CD4$^+$ T cells alone (2×10^6) were included as a control group. Development of diabetes was observed every other day for 40 days. Data were analyzed by Gehan-Breslow-Wilcoxon test. SPL, splenocytes.

agonists (Fig. 5A). We also measured cytokine production of the splenic DCs after stimulation with different TLR ligands. As shown in Fig. 5B, IRAK-M$^{-/-}$ NOD DCs secreted higher levels of IL-1β, IL-6, IL-12(p40), and IFN-γ following TLR ligation, especially with LPS. Again, DCs from IRAK-M$^{-/-}$ NOD mice secreted higher levels of those inflammatory cytokines in the absence of TLR ligation (Fig. 5B). TLR activation triggers downstream signaling pathways including the MAPK pathway (27) and NF-κB pathway (28), and there have been studies indicating that IRAK-M, the negative regulator of MyD88 signaling, is involved in the modulation of these pathways (6,29). To determine whether these signaling pathways were also affected in APCs of IRAK-M$^{-/-}$ NOD mice in response to TLR stimulation, we examined the activation of MAPK (Erk) and NF-κB (p65) in BMDCs from IRAK-M$^{-/-}$ NOD and WT NOD mice after LPS stimulation. It is interesting that DCs from IRAK-M$^{-/-}$ NOD mice showed increased phosphorylation of ERK1/2 (p42/p44), compared with

WT DCs, even without LPS stimulation (0 min; Fig. 5C). This was further increased after LPS stimulation (15–60 min) with a peak expression at 15 min, although the activation still persisted at 60 min when phosphorylation of ERK1/2 in DCs from WT NOD mice had been reduced to prestimulation level (Fig. 5C). Similarly, we found enhanced activation of NF-κB signaling, expressed by increased phosphorylation of p65 after LPS stimulation in DCs from IRAK-M$^{-/-}$ NOD mice compared with WT NOD mice, with a peak at 15 min (Fig. 5C). Different from the MAPK pathway, the NF-κB signaling appeared to be comparable between DCs from IRAK-M$^{-/-}$ and WT NOD mice at rest (time point 0 min; Fig. 5C). Taken together, IRAK-M deficiency upregulated costimulatory molecules and elevated inflammatory cytokine production in APCs, and this most likely occurred through the enhanced activation of MAPK and NF-κB signaling pathways.

To test the function of DCs in facilitating TCR cross-linking, we cocultured purified splenic CD4$^+$ and CD8$^+$
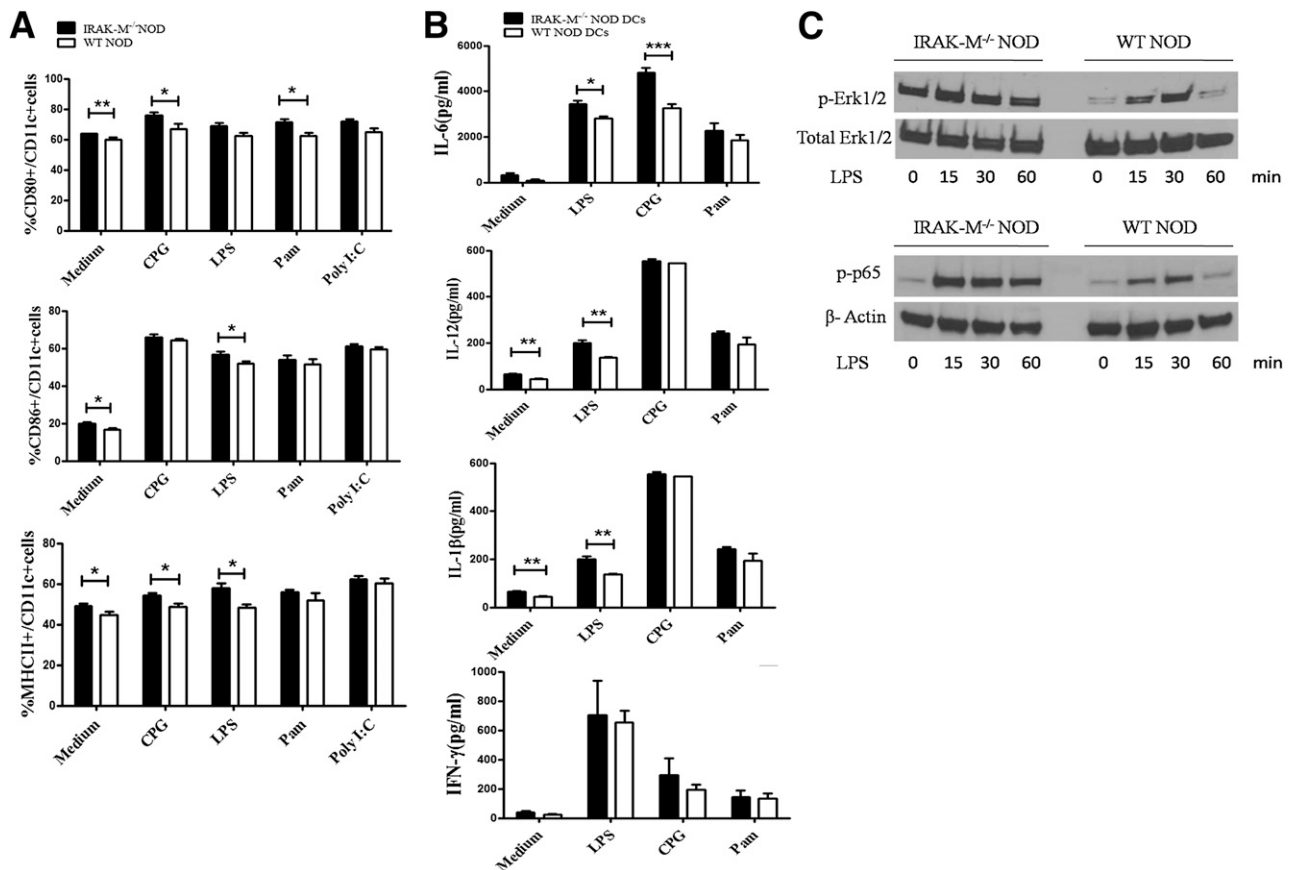
Figure 5—Increased cytokine production and activation of MAPK and NF-κB pathways in IRAK-M$^{-/-}$ DCs. A: Splenic CD11c^{+} DCs were treated or not treated with different TLR ligands (CpG 1 μg/mL; LPS 500 ng/mL; Pam$_3$CSK$_4$ 1 μg/mL; poly I:C 1 μg/mL) for 12 h, and the expression of CD80, CD86, and MHC class II on CD11c^{+} cells was investigated by flow cytometry. Data are presented as the percentage of CD80, CD86, and MHC class II–positive cells in total CD11c^{+}-gated cells. B: The supernatants from the cultures in A were tested for secreted IL-6, IL-12, IL-1β, and IFN-γ by Luminex or ELISA. Data were analyzed by Student t test (*P < 0.05; **P < 0.001; ***P < 0.0001). C: Western blot of phosphorylated ERK and p65. BMDCs from IRAK-M$^{-/-}$ NOD and WT mice were stimulated with or without LPS (1 μg/mL) for the indicated time. Cell lysates were prepared in the presence of protease and phosphatase inhibitors. Phospho-ERK, total ERK, phospho-p65, and actin (control) were blotted.

T cells from NOD mice with DCs (with or without pres-timulation by LPS) from IRAK-M$^{-/-}$ NOD or WT NOD mice in the presence of a low concentration of anti-CD3 mAbs. As shown in Fig. 6A, IRAK-M$^{-/-}$ NOD DCs enhanced the activation of both CD4^{+} and CD8^{+} T cells compared with WT DCs, and this was further enhanced if the DCs were prestimulated with LPS (Fig. 6A). To test whether IRAK-M$^{-/-}$ NOD DCs can directly affect cyto-kine production in effector T cells, we performed the same experiments, and examined IFN-γ and TNF-α producing CD4^{+} or CD8^{+} T cells at the end of a 4-day coculture. Consistent with the proliferation results, IRAK-M$^{-/-}$ NOD DCs promoted more CD4^{+} and CD8^{+} T cells to dif-ferentiate into IFN-γ and TNF-α producing Th1 and Tc1 cells, respectively, compared with WT DCs (Fig. 6B), and this stimulation was greater if DCs were preactivated with LPS (Fig. 6B). IFN-γ production in the coculture system was further confirmed by Luminex assay (Fig. 6C). In addition, the levels of IL-1β and IL-6, most likely produced by DCs, were also significantly higher in the cultures where

IRAK-M$^{-/-}$ NOD DCs were present (Fig. 6C). Our data demonstrated that IRAK-M$^{-/-}$ NOD DCs strongly affected effector T cells by enhancing their proliferation and pro-moting their differentiation into Th1 or Tc1 cells.

IRAK-M$^{-/-}$ DCs Heightened Antigen-Specific T-Cell Responses In Vitro and In Vivo

To test whether IRAK-M$^{-/-}$ NOD DCs could also induce robust immune responses to a diabetes-irrelevant antigen, we immunized WT NOD mice with KLH. Splenic CD4^{+} and CD8^{+} T cells were purified from the immunized mice 7 days after immunization and cocultured with pu-rified naive IRAK-M$^{-/-}$ NOD DCs or WT NOD DCs that had or had not been preloaded with KLH. Untreated DCs were used as controls. As shown in Fig. 7A, the KLH-specific T-cell responses were much stronger (determined by ^{3}H-thymidine incorporation) when IRAK-M$^{-/-}$ NOD DCs were used as APCs. This suggests that IRAK-M$^{-/-}$ DCs can induce more robust antigen-specific T-cell responses generally. To further confirm the finding, we
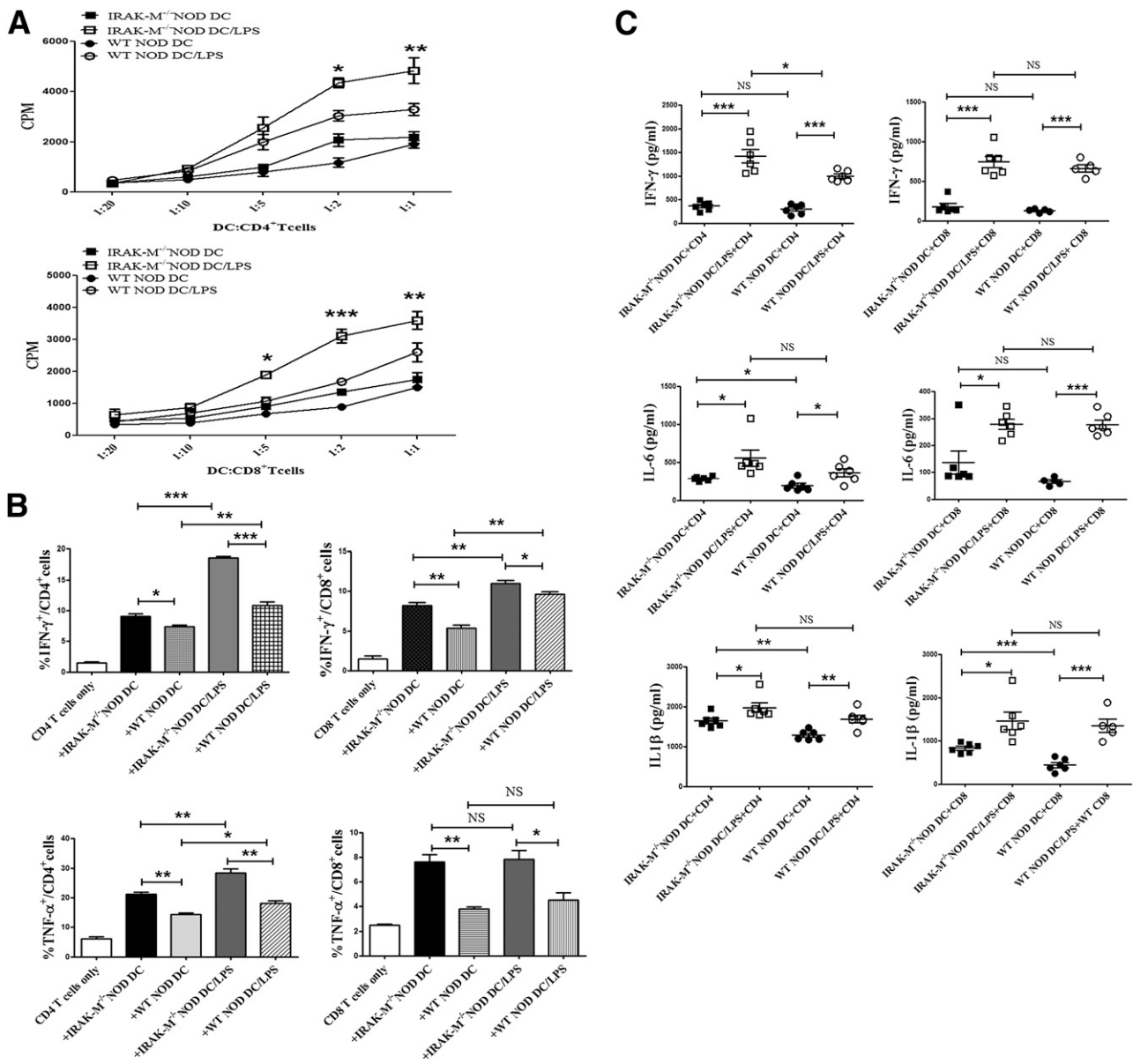
Figure 6—IRAK-M$^{-/-}$ NOD DCs activate diabetogenic T cells more effectively with increased proliferation and cytokine production than WT NOD DCs. *A*: IRAK-M$^{-/-}$ NOD DCs significantly enhanced T-cell proliferation in vitro. Splenic DCs from IRAK-M$^{-/-}$ NOD or WT NOD mice were pretreated or untreated with LPS (4 h, 37°C) and cocultured with bead-purified splenic CD4$^+$ or CD8$^+$ T cells at different ratios with a low dose of anti-CD3 antibody (1:300 dilution of 2C11 hybridoma supernatant) for 5 days. ^{3}H-Thymidine was added to the coculture system during the last 16 h. T-cell proliferation was measured by ^{3}H-thymidine incorporation. Two-way ANOVA was used for statistical analysis (*P < 0.05; **P < 0.001; ***P < 0.0001). *B*: Purified NOD spleen T cells (CD4$^+$ or CD8$^+$) were cocultured with IRAK-M$^{-/-}$ NOD or WT NOD DCs (LPS-treated or not) for 4 days (T cell/DC ratio 2:1) with a low dose (1:300) of anti-CD3 antibody. Cells were then stained for intracellular IFN-γ and TNF-α (gated on CD4$^+$ and CD8$^+$ populations). A summary of the percentage of IFN-γ (top) or TNF-α (bottom) expressing CD4$^+$ and CD8$^+$ T cells is shown. IRAK-M$^{-/-}$ NOD DCs increased the production of IFN-γ in T cells, compared with WT NOD DCs. Data are representative of three individual experiments. *C*: Supernatants from the T-cell and DC coculture system (T/DC ratio 2:1) were collected, and the levels of IFN-γ, IL-1β, and IL-6 were determined by Luminex assay. Consistent with the flow cytometric results, the increased production of all three inflammatory cytokines was more significant in the cultures with IRAK-M$^{-/-}$ NOD DCs than in those with WT NOD DCs. Data were analyzed by Student t test. *P < 0.05; **P < 0.001; ***P < 0.0001. CPM, counts per minute.

conducted an in vivo experiment, in which we gave a single dose (10^6/mouse) of IRAK-M$^{-/-}$ NOD DCs or WT NOD DCs preloaded with KLH by intravenous injection to WT NOD mice. We harvested splenocytes from the DC-treated mice 7 days after injection and performed proliferation assays in response to KLH stimulation. Supporting our

results shown in Fig. 7*A*, splenocytes from the IRAK-M$^{-/-}$ NOD DC-vaccinated mice also showed significantly higher antigen-specific proliferation to KLH stimulation compared with splenocytes from the WT NOD DC-vaccinated control mice (Fig. 7*B*). Taken together, our results from the two sets of experiments demonstrated that DCs
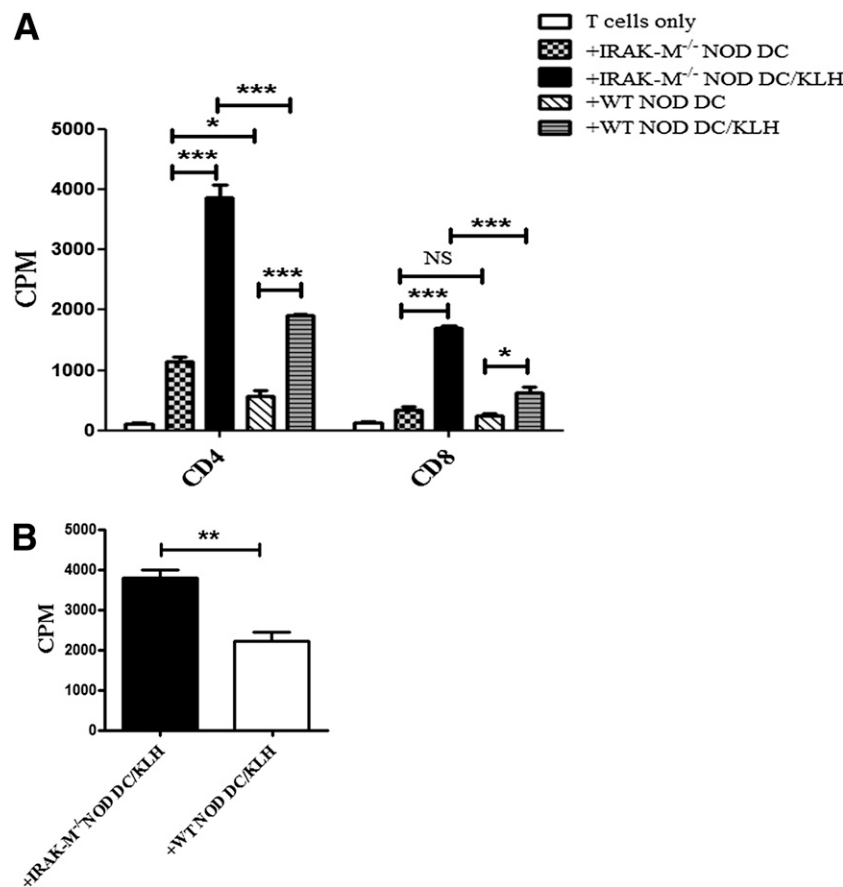
Figure 7—IRAK-M$^{-/-}$ NOD DCs enhanced antigen-specific T-cell response in vitro and in vivo. *A*: WT NOD mice were immunized with KLH (200 μg/mice i.p.). Splenic CD4$^+$ and CD8$^+$ T cells were purified 7 days after immunization. Splenic DCs from naive IRAK-M$^{-/-}$ NOD or WT NOD mice were or were not preloaded with KLH (50 μg/mL) for 5 h at 37°C and further cocultured with CD4$^+$ or CD8$^+$ T cells from immunized mice for 5 days. ^{3}H-Thymidine incorporation assays were performed to test T-cell proliferation. *B*: Splenic DCs purified from naive IRAK-M$^{-/-}$ NOD or WT NOD mice were loaded with KLH protein (50 μg/mL for 5 h at 37°C) and injected intravenously into 2-month-old female NOD mice (*n* = 3 mice/group). Splenocytes were harvested from the immunized mice 7 days later and cultured in vitro in the presence of 1 μg/mL KLH for 5 days. ^{3}H-Thymidine incorporation was measured. Data represent two separate experiments and were analyzed by Student *t* test. *P < 0.05; **P < 0.001; ***P < 0.0001. CPM, counts per minute.

lacking IRAK-M expression were highly efficient APCs both in vivo and in vitro. Our data also suggest that IRAK-M$^{-/-}$ NOD DCs could be used in a vaccination approach to induce strong antigen-specific T-cell responses.

IRAK-M$^{-/-}$ NOD DCs Enhanced Diabetogenic BDC-2.5 CD4$^+$ T-Cell Responses In Vivo and In Vitro

To test whether IRAK-M$^{-/-}$ NOD DCs can enhance the function of diabetogenic BDC-2.5 T-cell responses, we first cocultured purified BDC-2.5 CD4$^+$ T cells with DCs from IRAK-M$^{-/-}$ NOD or WT NOD mice in the presence of a BDC-2.5 mimotope peptide. As expected, IRAK-M$^{-/-}$ NOD DCs showed superior antigen presentation by inducing a significantly higher proliferation of BDC-2.5 CD4$^+$ T cells (Fig. 8*A*). To study the function of DCs in vivo, we intravenously injected BDC-2.5 mimotope peptide preloaded DCs (10^6/mouse) from IRAK-M$^{-/-}$ NOD or WT NOD mice into BDC-2.5 NOD mice. Splenocytes from the recipients were harvested 7 days after the DC

injection, and we examined both phenotype and function. We found that a higher percentage of CD4$^+$ T cells from BDC-2.5 transgenic mice that received IRAK-M$^{-/-}$ NOD DCs expressed effector/memory markers (CD44^{hi}/CD62L^{lo}) compared with CD4 T cells from mice that were given WT NOD DCs (Fig. 8*B*). We also found a reduction in the percentage of naive BDC-2.5 CD4$^+$ T cells (CD44^{lo}/CD62L^{hi}) in the recipients that received IRAK-M$^{-/-}$ DCs compared with those that were injected with WT DCs, but this was not statistically significant (Fig. 8*B*). We further examined expression of the activation marker CD69 on T cells of both groups and found a higher expression of CD69 on T cells in IRAK-M$^{-/-}$ NOD DC–vaccinated mice compared with T cells from WT NOD DC–vaccinated mice (Fig. 8*C*). Furthermore, more IFN-γ–producing BDC-2.5 CD4$^+$ T cells were found in IRAK-M$^{-/-}$ NOD DC–vaccinated mice compared with WT NOD DC–vaccinated mice (Fig. 8*C*). Consistent with the IFN-γ results, there was also a higher frequency of T-bet$^+$
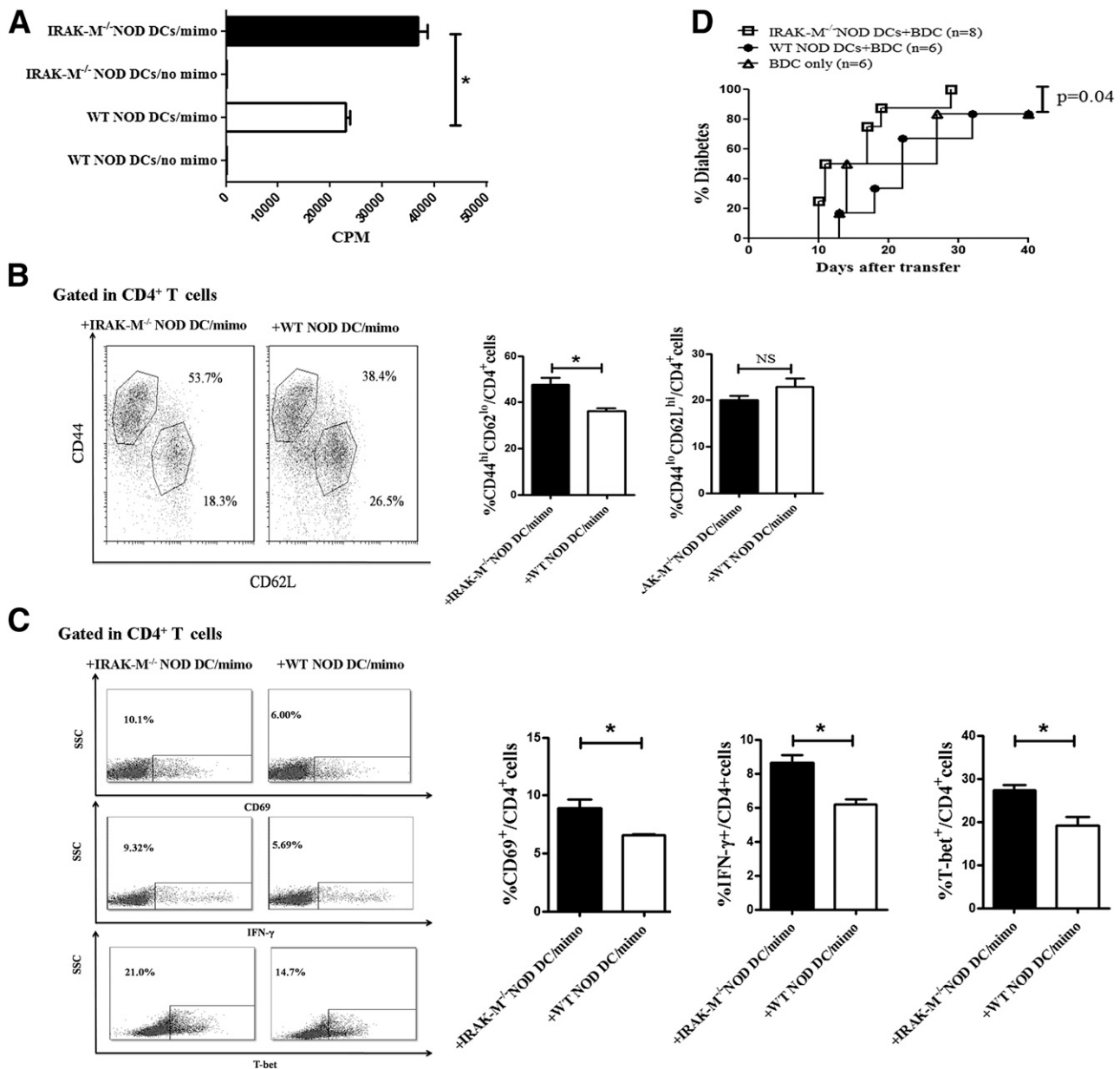
Figure 8—Increased pathogenicity of diabetogenic CD4 T cells in the presence of IRAK-M$^{-/-}$ NOD DCs in vivo. *A*: The antigen-presenting function of splenic DCs from IRAK-M$^{-/-}$ NOD and WT NOD mice was tested by coculturing the DCs with 5×10^4/well purified BDC-2.5 CD4$^+$ T cells (T/DC ratio 2:1) in the presence of BDC-2.5 mimotope (mimo; 10 ng/mL) for 5 days. Proliferation of BDC-CD4$^+$ T cells with IRAK-M$^{-/-}$ NOD DCs or WT NOD DCs without mimotope were used as controls. ^{3}H-Thymidine incorporation was used to assess antigen-specific T-cell proliferation. Student *t* test was used for statistical analysis (*P < 0.05). *B*: Splenic DCs from IRAK-M$^{-/-}$ NOD and WT NOD mice were loaded with 500 ng/mL BDC-2.5 mimotope for 5 h and washed before intravenous transfer into BDC-2.5 transgenic mice (female, 8 weeks old, *n* = 3/group). Mice were killed 7 days after DC injection and splenocytes were harvested for surface marker analysis. CD44^{high}CD62L^{low} effector/memory CD4$^+$ T cells were significantly increased in the recipient BDC-2.5 mice that received IRAK-M$^{-/-}$ NOD DC pulsed with BDC-2.5 mimotope compared with the control group. The left panel shows representative dot plots for CD44 and CD62L staining in gated CD4$^+$ T cells. The bar charts on the right summarized the percentage of effector/memory (CD44^{high}CD62L^{low}) and naive (CD44^{low}CD62L^{high}) subsets in CD4$^+$ T cells. Student *t* test was used for statistical analysis (*P < 0.05). NS, not significant. *C*: Splenocytes from the recipient BDC-2.5 mice were examined for other markers. Dot plots of CD69, IFN-γ, and T-bet expression in gated CD4$^+$ T cells are shown on the left, and the bar chart summary is shown on the right. Data were analyzed by Student *t* test (*P < 0.05). *D*: Splenic DCs from IRAK-M$^{-/-}$ NOD or WT NOD mice were preloaded with 500 ng/mL BDC-2.5 mimotope for 5 h and cotransferred (after washing, 10^6/mouse) with 2×10^6 purified BDC-2.5 CD4$^+$ T cells into NOD.SCID mice (4–5 weeks old, *n* = 6–8/group). NOD.SCID mice (4–5 weeks old, *n* = 6) that received 2×10^6 BDC-CD4$^+$ T cells alone were used as controls. The incidence of diabetes was monitored every other day for a total 40 days, and statistical analysis was performed with the Gehan-Breslow-Wilcoxon test.

BDC-2.5 CD4$^+$ T cells in IRAK-M$^{-/-}$ NOD DC–vaccinated mice (Fig. 8C). To test whether IRAK-M$^{-/-}$ NOD DCs can enhance the diabetogenicity of BDC-2.5 CD4$^+$ T cells, we adoptively transferred BDC-2.5 mimotope-pulsed IRAK-M$^{-/-}$ NOD DCs or WT NOD DCs (10^6/mouse), together with an equal number of purified BDC-2.5 CD4$^+$ T cells to NOD.SCID mice. As shown in Fig. 8D, NOD.SCID mice that received IRAK-M$^{-/-}$ NOD DCs developed accelerated diabetes compared with the NOD.SCID mice that received WT NOD DCs (P = 0.04). To show that the accelerated diabetes was not related to influence by endogenous APCs like DCs or macrophages in SCID recipients in this adoptive transfer model, we injected an additional group of NOD.SCID mice with an equal number of purified BDC-2.5 CD4$^+$ T cells only. Although the incidence of diabetes in this control group was similar to that in the group that was cotransferred with WT DCs, there was no significant difference when compared with the group that was coinjected with IRAK-M$^{-/-}$ DCs (Fig. 8D).

DISCUSSION

In this study, we have shown that IRAK-M plays an inhibitory role in the development of autoimmune diabetes in NOD mice. This was shown by accelerated development of the disease in IRAK-M$^{-/-}$ NOD mice, in both spontaneous and induced models, with impaired glucose tolerance, increased numbers of circulating anti-IAAs, and more infiltrated islets compared with WT NOD littermates. In addition, we demonstrated superior function of DCs from IRAK-M$^{-/-}$ NOD mice, which promoted an increased proportion of effector/memory T cells, increased their proliferation and inflammatory cytokine production, and enhanced the diabetogenicity of autoreactive T cells.

The innate immune system senses invading microbes and pathogens through TLRs, and signaling through these receptors subsequently induces the production of proinflammatory cytokines and chemokines to control infection (3,30,31). TLRs transduce their signals through either MyD88 (32), which is used by most of the TLRs, or TRIF (33), which regulates TLR3 signaling and, partially, TLR4 signaling. Increasing evidence suggests that TLRs also sense endogenous ligands including self-antigens (34–36). We previously reported that MyD88$^{-/-}$ NOD mice were completely protected from T1DM when animals were housed in specific pathogen-free conditions (19), which suggests that MyD88, the major TLR downstream signaling molecule, is essential for T1DM development under specific pathogen-free housing conditions. IRAK-M negatively regulates MyD88 signals to prevent the activation of downstream NF-κB and the production of inflammatory cytokines (37). It is conceivable that in the absence of this negative regulator, MyD88 might be overactivated and lead to an unbalanced inflammatory immune response. Our previous study using MyD88$^{-/-}$ NOD mice suggests an intimate three-way relationship among commensal bacteria, MyD88, and T1DM development (19). The commensal bacteria have an effect that is detected by the immune system signaling through MyD88. However, the host immune system also has an effect on the composition of the microbiome. It is not clear at this stage whether IRAK-M also affects the gut microbiome, which may regulate T1DM development.

In addition to its expression in macrophages, DCs (6,23), B cells (24), and neutrophils (38), IRAK-M is also expressed in liver (39) and lung epithelial cells (40). We examined freshly isolated islet β-cells and did not find IRAK-M expression (data not shown). Thus, IRAK-M deficiency is unlikely to directly affect islet β-cell function. However, by using a stepwise approach, we showed that in the absence of IRAK-M, a higher proportion of DCs, in the steady state, expressed an activated phenotype and a typical DC1 cytokine profile (41). This in turn promoted increased diabetogenic T-cell proliferation and Th1 differentiation, which led to rapid progression to development of T1DM. Our results indicate that IRAK-M, particularly in DCs, is important in controlling islet autoimmunity in NOD mice.

In mechanistic terms, upon TLR ligation, IRAK-M negatively regulates the MyD88 pathways by preventing the dissociation of IRAK-1/2 from the MyD88-IRAK-4-TRAF6 complex (37), thereby limiting the activation of NF-κB and MAP kinase signaling pathways, which initiate downstream proinflammatory cytokine cascades (29,42). Indeed, we found that, in the absence of IRAK-M, DCs have elevated and prolonged phosphorylation of ERK (MAPK) and p65 (NF-κB). In the absence of IRAK-M, more DCs and macrophages also displayed an activated phenotype by upregulation of costimulatory markers and MHC class II molecule expression. This was further enhanced upon TLR ligation. DCs and macrophages have been classified as DC1/DC2 and M1/M2, respectively, according to the cytokine profile they produce (43,44). In the absence of IRAK-M, DCs and macrophages showed a predominant DC1 and M1 phenotype, namely, expressing higher levels of IL-12 and IFN-γ. We found that not only were IRAK-M$^{-/-}$ NOD DCs superior in producing proinflammatory cytokines, preferentially promoting IFN-γ–secreting Th1 cells, but they also potently presented antigens to diabetogenic T cells. This led to higher T-cell responses, inflammatory cytokine secretion, and islet β-cell destruction. Unregulated activation of innate immunity, such as through TLRs, is undesirable as TLR activation leads to inflammatory responses, which, if uncontrolled, may precipitate autoimmune responses. Studies (45–47) have shown that inactivation of TLRs can prevent experimental autoimmune disorders. However, other studies (48) also demonstrated that the inactivation of TLRs, in particular TLR9, can exacerbate autoimmunity, such as occurs in lupus. It is interesting that studies in NOD mice (49,50) showed that the activation of MyD88-independent TLR3 or partially MyD88-dependent TLR4 could prevent diabetes development. We and others reported that the inactivation of MyD88-dependent TLR2 protects NOD mice from diabetes development (18,19); however, it appeared that the activation of TLR2 also

protect NOD mice from diabetes development, possibly because of TLR2 tolerization by repeated stimulation (51). Our study supports the notion that uncontrolled TLR activation and the activation of downstream MyD88 signaling pathways through removing a major negative regulator, IRAK-M, is detrimental to the susceptible host, as removing IRAK-M accelerated the onset of diabetes. Although other studies have shown that IRAK-M has a direct effect on TLR2, 4, 7, and 9 (52,53), it is not clear whether IRAK-M can directly regulate the function of TLRs in our model system. However, we found that ligation of TLRs, in particular LPS, further enhanced the activated phenotype and function of DCs and macrophages in the absence of IRAK-M.

The accelerated diabetes development seen in IRAK-M$^{-/-}$ NOD mice is characterized by earlier disease onset and rapid progression of diabetes. The early diabetes onset in IRAK-M$^{-/-}$ NOD mice was in evidence until 20 weeks of age, when ~80% of IRAK-M$^{-/-}$ mice had developed diabetes, whereas only ~45% of IRAK-M–sufficient mice were diabetic at the same time point. It is interesting that none of the IRAK-M mice we observed developed diabetes after 20 weeks, whereas IRAK-M–sufficient mice continued to develop diabetes. This suggests that the effects of the innate immune pathway in influencing disease are most important in the early phases of disease pathogenesis. The effects of environmental stimuli are likely to be mediated through the innate immune receptors, and it has been reported that early rather than later exposure to viral infection has more of an effect on the delay and prevention of T1DM in the NOD mouse model (54). Our data implicate the innate pathways as having an effect early in the course of the disease and emphasize the likely influence that early environment plays on the diabetes development. This may be particularly important as recent studies have indicated that the increased incidence of T1DM in younger children relates to accelerated progression from islet autoimmunity to the development of clinical diabetes (55).

In summary, our data suggest IRAK-M, a negative regulator of innate immunity through TLR/MyD88, plays an important role in T1DM development, which is most likely mediated by APCs and, in particular, DCs. This study opens a new view of how TLRs and the innate system, especially the MyD88 pathway, are involved in the pathogenesis of the disease. Knowledge of the factors that may enhance or diminish the negative regulation of these major pathways controlling innate immune responses will be important in increasing our understanding of how the environment influences the development of autoimmune diabetes. Ultimately, finding ways of boosting this negative regulation, especially early in life, may be very important in the delay or prevention of T1DM.

References
1. Akira S, Uematsu S, Takeuchi O. Pathogen recognition and innate immunity. Cell 2006;124:783–801
2. Medzhitov R. Recognition of microorganisms and activation of the immune response. Nature 2007;449:819–826
3. Medzhitov R, Preston-Hurlburt P, Janeway CA Jr. A human homologue of the Drosophila Toll protein signals activation of adaptive immunity. Nature 1997; 388:394–397
4. Marshak-Rothstein A. Toll-like receptors in systemic autoimmune disease. Nat Rev Immunol 2006;6:823–835
5. Iwasaki A, Medzhitov R. Toll-like receptor control of the adaptive immune responses. Nat Immunol 2004;5:987–995
6. Kobayashi K, Hernandez LD, Galán JE, Janeway CA Jr, Medzhitov R, Flavell RA. IRAK-M is a negative regulator of Toll-like receptor signaling. Cell 2002;110:191–202
7. Flannery S, Bowie AG. The interleukin-1 receptor-associated kinases: critical regulators of innate immune signalling. Biochem Pharmacol 2010;80: 1981–1991
8. Turnis ME, Song XT, Bear A, et al. IRAK-M removal counteracts dendritic cell vaccine deficits in migration and longevity. J Immunol 2010;185:4223–4232
9. Tazi KA, Quioc JJ, Saada V, Bezeaud A, Lebrec D, Moreau R. Upregulation of TNF-alpha production signaling pathways in monocytes from patients with advanced cirrhosis: possible role of Akt and IRAK-M. J Hepatol 2006;45:280–289
10. Balaci L, Spada MC, Olla N, et al. IRAK-M is involved in the pathogenesis of early-onset persistent asthma. Am J Hum Genet 2007;80:1103–1114
11. Wiersinga WJ, van't Veer C, van den Pangaart PS, et al. Immunosuppression associated with interleukin-1R-associated-kinase-M upregulation predicts mortality in Gram-negative sepsis (melioidosis). Crit Care Med 2009;37:569–576
12. Hoogerwerf JJ, van der Windt GJ, Blok DC, et al. Interleukin-1 receptor-associated kinase M-deficient mice demonstrate an improved host defense during Gram-negative pneumonia. Mol Med 2012;18:1067–1075
13. Weersma RK, Oostenbrug LE, Nolte IM, et al. Association of interleukin-1 receptor-associated kinase M (IRAK-M) and inflammatory bowel diseases. Scand J Gastroenterol 2007;42:827–833
14. Berglund M, Melgar S, Kobayashi KS, Flavell RA, Hörnquist EH, Hultgren OH. IL-1 receptor-associated kinase M downregulates DSS-induced colitis. Inflamm Bowel Dis 2010;16:1778–1786
15. Lech M, Kantner C, Kulkarni OP, et al. Interleukin-1 receptor-associated kinase-M suppresses systemic lupus erythematosus. Ann Rheum Dis 2011;70:2207–2217
16. Wong FS, Janeway CA Jr. The role of CD4 and CD8 T cells in type I diabetes in the NOD mouse. Res Immunol 1997;148:327–332
17. Babaya N, Nakayama M, Eisenbarth GS. The stages of type 1A diabetes. Ann N Y Acad Sci 2005;1051:194–204
18. Kim HS, Han MS, Chung KW, et al. Toll-like receptor 2 senses beta-cell death and contributes to the initiation of autoimmune diabetes. Immunity 2007; 27:321–333

19. Wen L, Ley RE, Volchkov PY, et al. Innate immunity and intestinal microbiota in the development of Type 1 diabetes. Nature 2008;455:1109–1113

20. Meyers AJ, Shah RR, Gottlieb PA, Zipris D. Altered Toll-like receptor signaling pathways in human type 1 diabetes. J Mol Med (Berl) 2010;88:1221–1231

21. Zhang Y, Lee AS, Shameli A, et al. TLR9 blockade inhibits activation of diabetogenic CD8+ T cells and delays autoimmune diabetes. J Immunol 2010; 184:5645–5653

22. Tai N, Wong FS, Wen L. TLR9 deficiency promotes CD73 expression in T cells and diabetes protection in nonobese diabetic mice. J Immunol 2013;191: 2926–2937

23. Wesche H, Gao X, Li X, Kirschning CJ, Stark GR, Cao Z. IRAK-M is a novel member of the Pelle/interleukin-1 receptor-associated kinase (IRAK) family. J Biol Chem 1999;274:19403–19410

24. Meyer-Bahlburg A, Khim S, Rawlings DJ. B cell intrinsic TLR signals amplify but are not required for humoral immunity. J Exp Med 2007;204:3095–3101

25. Stadinski BD, Delong T, Reisdorph N, et al. Chromogranin A is an auto-antigen in type 1 diabetes. Nat Immunol 2010;11:225–231

26. Ganguly D, Haak S, Sisirak V, Reizis B. The role of dendritic cells in au-toimmunity. Nat Rev Immunol 2013;13:566–577

27. Dong C, Davis RJ, Flavell RA. MAP kinases in the immune response. Annu Rev Immunol 2002;20:55–72

28. Zhang G, Ghosh S. Toll-like receptor-mediated NF-kappaB activation: a phylogenetically conserved paradigm in innate immunity. J Clin Invest 2001; 107:13–19

29. Janssens S, Beyaert R. Functional diversity and regulation of different in-terleukin-1 receptor-associated kinase (IRAK) family members. Mol Cell 2003;11: 293–302

30. Hemmi H, Takeuchi O, Kawai T, et al. A Toll-like receptor recognizes bacterial DNA. Nature 2000;408:740–745

31. Rock FL, Hardiman G, Timans JC, Kastelein RA, Bazan JF. A family of human receptors structurally related to Drosophila Toll. Proc Natl Acad Sci USA 1998;95:588–593

32. Wesche H, Henzel WJ, Shillinglaw W, Li S, Cao Z. MyD88: an adapter that recruits IRAK to the IL-1 receptor complex. Immunity 1997;7:837–847

33. Yamamoto M, Sato S, Hemmi H, et al. Role of adaptor TRIF in the MyD88-independent toll-like receptor signaling pathway. Science 2003;301:640–643

34. Lau CM, Broughton C, Tabor AS, et al. RNA-associated autoantigens acti-vate B cells by combined B cell antigen receptor/Toll-like receptor 7 engagement. J Exp Med 2005;202:1171–1177

35. Hurst J, von Landenberg P. Toll-like receptors and autoimmunity. Auto-immun Rev 2008;7:204–208

36. Guiducci C, Gong M, Xu Z, et al. TLR recognition of self nucleic acids hampers glucocorticoid activity in lupus. Nature 2010;465:937–941

37. Deng L, Wang C, Spencer E, et al. Activation of the IkappaB kinase complex by TRAF6 requires a dimeric ubiquitin-conjugating enzyme complex and a unique polyubiquitin chain. Cell 2000;103:351–361

38. Hubbard LL, Ballinger MN, Thomas PE, et al. A role for IL-1 receptor-as-sociated kinase-M in prostaglandin E2-induced immunosuppression post-bone marrow transplantation. J Immunol 2010;184:6299–6308

39. Harada K, Nakanuma Y. Biliary innate immunity and cholangiopathy. Hep-atol Res 2007;37(Suppl. 3):S430–S437

40. Lagler H, Sharif O, Haslinger I, et al. TREM-1 activation alters the dynamics of pulmonary IRAK-M expression in vivo and improves host defense during pneumococcal pneumonia. J Immunol 2009;183:2027–2036

41. Bottomly K. T cells and dendritic cells get intimate. Science 1999;283: 1124–1125

42. Rosati O, Martin MU. Identification and characterization of murine IRAK-2. Biochem Biophys Res Commun 2002;297:52–58

43. Liu YJ. Dendritic cell subsets and lineages, and their functions in innate and adaptive immunity. Cell 2001;106:259–262

44. Sica A, Mantovani A. Macrophage plasticity and polarization: in vivo veritas. J Clin Invest 2012;122:787–795

45. Pierer M, Wagner U, Rossol M, Ibrahim S. Toll-like receptor 4 is involved in inflammatory and joint destructive pathways in collagen-induced arthritis in DBA1J mice. PLoS One 2011;6:e23539

46. Prinz M, Garbe F, Schmidt H, et al. Innate immunity mediated by TLR9 modulates pathogenicity in an animal model of multiple sclerosis. J Clin Invest 2006;116:456–464

47. Reynolds JM, Pappu BP, Peng J, et al. Toll-like receptor 2 signaling in CD4(+) T lymphocytes promotes T helper 17 responses and regulates the pathogenesis of autoimmune disease. Immunity 2010;32:692–702

48. Nickerson KM, Cullen JL, Kashgarian M, Shlomchik MJ. Exacerbated au-toimmunity in the absence of TLR9 in MRL.Fas(lpr) mice depends on Ifnar1. J Immunol 2013;190:3889–3894

49. Serreze DV, Hamaguchi K, Leiter EH. Immunostimulation circumvents diabetes in NOD/Lt mice. J Autoimmun 1989;2:759–776

50. Aumeunier A, Grela F, Ramadan A, et al. Systemic Toll-like receptor stimulation suppresses experimental allergic asthma and autoimmune diabetes in NOD mice. PLoS One 2010;5:e11484

51. Kim DH, Lee JC, Kim S, et al. Inhibition of autoimmune diabetes by TLR2 tolerance. J Immunol 2011;187:5211–5220

52. Hatao F, Yamamoto M, Muroi M, Kaminishi M, Tanamoto K. MyD88-induced downregulation of IRAK-4 and its structural requirements. FEMS Immunol Med Microbiol 2008;53:260–264

53. Zhou H, Yu M, Fukuda K, et al. IRAK-M mediates Toll-like receptor/IL-1R-induced NFκB activation and cytokine production. EMBO J 2013;32:583–596

54. Filippi CM, Estes EA, Oldham JE, von Herrath MG. Immunoregulatory mechanisms triggered by viral infections protect from type 1 diabetes in mice. J Clin Invest 2009;119:1515–1523

55. Ziegler AG, Pflueger M, Winkler C, et al. Accelerated progression from islet autoimmunity to diabetes is causing the escalating incidence of type 1 diabetes in young children. J Autoimmun 2011;37:3–7